

NEW COMPUTER CODES FOR THE STRUCTURAL ANALYSIS OF COMPOSITE HELICOPTER STRUCTURES

Helmut Rapp
Messerschmitt-Bölkow-Blohm GmbH
Helicopter Division
München, Germany

Abstract

Helicopters of the new generation will show a very high portion of structural components made of fiber composites. To take the best advantage of these materials modern tools for structural design and analysis are necessary. With methods of structural optimization at panel level, already in early design phases the best fiber orientation and laminate thicknesses can be chosen. By means of a helicopter fuselage sidewall and a sandwich panel of the horizontal stabilizer it is shown that large weight savings can be achieved with optimal laminates. Combination of composite materials with very different Poisson's ratios in barlike components result in additional stresses perpendicular to the load direction, which may have a noticeable influence on the tension and bending stiffness. The basic theory is given and a special test-bar shows the large influence these stresses may have. Investigations of a helicopter rotor blade as a typical application of such a non-homogeneous structural part, however, shows that in this case the influence of the additional stresses is small.

In future helicopter projects often thickwalled composite parts for rotor components are used. The stress and stiffness evaluation of such components require a finite element analysis. To reduce the necessary effort a computer code was developed to determine the material properties of a thick laminate and to evaluate the stresses in a single layer of this laminate due to membrane and bending forces.

1. Introduction

In actual and in new helicopter projects fiber reinforced materials play an important role for structural components. Nearly all load transferring structures are made of such materials, only in areas, which are loaded by higher temperatures, conventional isotropic metals are used. In the current MBB projects PAH/HAC [1] and BO108 [2] the airframe structures are mostly made from carbon and aramid fiber reinforced materials. For both helicopters advanced rotor concepts are used. The hub of the PAH/HAC FEL rotor (fiber-elastomer rotor) mainly consists of two thick carbon fiber plates while the BO108 rotor is a bearingless rotor made from glass and carbon fiber reinforced materials.

Due to the anisotropic character of the FRP materials, the analysing of such structures is very demanding. The

necessary tools as theories and computer codes have to describe the essential problems correctly and beside this they have to be very reliable and easy to use.

In recent years, three new computer codes have been developed which deal with special problems of analysing and designing structures made out of fiber reinforced material. These modern tools make it possible to develop and design structures for new helicopters with higher quality in a shorter time than it was some years ago.

In this context, especially the structural optimization must be mentioned. In the field of structural optimization, there exist two principle approaches: First the whole structure can globally be optimized by using one of the great computer codes based on the finite element theory (e.g. MBB-Lagrange, MSC-NASTRAN, etc.). Second, it can also be useful to analyse special components or parts of structures by means of small computer codes which also make use of methods of numerical optimization. OLGA is one of these small codes for the optimization of fiber reinforced laminates at panel level. Single layer thicknesses and fiber orientation angles are varied in such a manner that optimal stiff and light laminates are achieved under consideration of certain design constraints.

Another area of interest is the analysis of non-homogeneous barlike structures like rotor blades. In such parts the different materials influence each other in their deformation due to different Poisson's ratios. Additional stresses, which are usually neglected in the engineering theory of bending, may have a noticeable influence on the tension- and bending stiffness and also on the coefficient of thermal expansion. This influence can be determined by the use of the code SABINA. It allows the evaluation of the effective stiffnesses and coefficients of thermal expansion by calculating the additional stresses.

For the structural analysis of thickwalled structures the finite element method is necessary. To simplify such a three dimensional analysis the computer code ETHERM3D was developed. The underlying theory is an expansion of the classical laminate theory. With this theory all three dimensional effective moduli of any multi-layered laminate can be evaluated. Therefore it is no longer necessary to idealize each single layer. Combining some layers of a thick laminate to a new material with special properties considerably reduces the effort of

idealizing a three dimensional structure.

2. Structural Optimization at Panel Level

When designing helicopter parts such as fuselages or stabilizers one is faced with the question of what lay-up shall be used for the different laminates. In general laminates of the $(0^\circ/90^\circ/\pm 45^\circ)$ family are used. But are they really the right selection in all cases? To answer this question it is useful to have a computer code which supports the designer in the selection of the best laminate for a special application. So, already in early phases of a project, a good design can be achieved.

2.1 General Remarks

The code OLGA (*Optimierung von Laminaten mit Geschichtetem Aufbau*, which means: optimization of laminates with a layered structure) is based on the classical laminate theory and uses a numerical optimizer working with the method of the interior penalty function. With the aid of OLGA it is possible to determine the optimal lay-up for any laminate (figure 1) under nearly any design constraints.

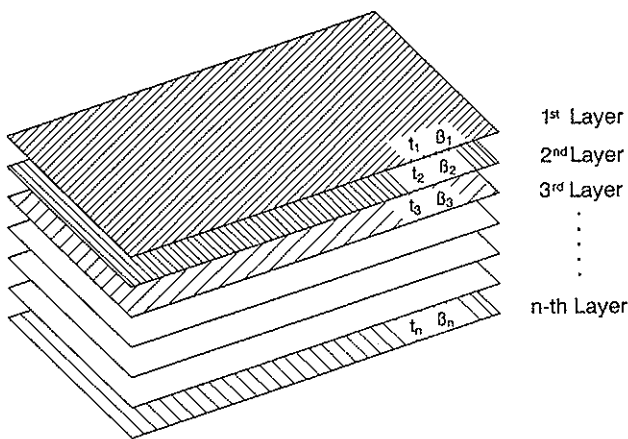


Figure 1: Geometry of general laminate

As design variables the thickness t and the fiber orientation angle β of any layer of the laminate can be chosen. The vector of the design variables $[x]$ has the form

$$[x] = [t_1, \dots, t_n, \beta_1, \dots, \beta_n]^T.$$

For a laminate with n layers the vector $[x]$ can contain up to n layer thicknesses and n fiber orientation angles. In general, however, the number of design variables will be less. Layer thicknesses and fiber angles respectively can be linked together either to reduce the number of design variables or to achieve a special form of lay-up (for instance for a symmetric or an orthotropic laminate). The linking is accomplished by the linking matrix $[L]$, which connects the set of design variables $[x]$ with the real laminate thicknesses t_j and fiber orientation angles β_j :

$$[t_1, \dots, t_n, \beta_1, \dots, \beta_n]^T = [L][x].$$

The quantity to be optimized (i.e. maxi- or minimized) is called the objective function. This objective function

is given as an explicit or implicit function of the design variables. In OLGA as objective function any result of the classical laminate theory can be chosen. Especially the weight and the laminate stiffnesses (Young's moduli, shear moduli, coefficients of the stiffness matrix, etc.) can be maxi- or minimized. It is also possible to combine some results to a new function, which then will be optimized.

The design constraints can also be any result of the laminate theory, especially the laminate strength (stresses in the single layers and factors of safety respectively, evaluated by application of a proper failure criterion such as that from Tsai-Wu), the laminate stiffness (again moduli or coefficients of the stiffness matrix) or the temperature expansion of the laminate. Up to ten loadcases can be considered for the optimization. Again it is possible to combine some results of the laminate theory to get further constraint functions. Additional to the standard output of the classical laminate theory an extension for the treatment of face sheet wrinkling of sandwich structures was carried out. So, also this kind of local instability may be used as design constraint. A future extension will deal with the global stability of rectangular plates.

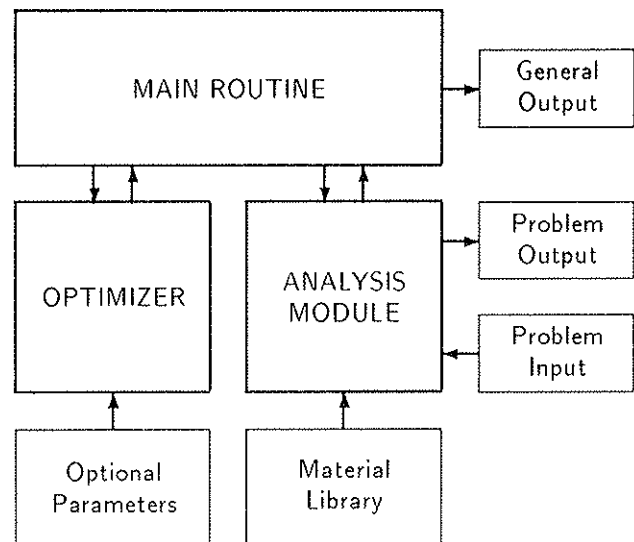


Figure 2: The structure of OLGA

Figure 2 shows the structure of OLGA. It consists of three routines, the main program, the analysis module and the optimizer. The clear structure of the program allows it to make extensions, concerning additional objective functions or design constraints very fast.

The input data for OLGA consist of two datasets. One contains special control parameters for the optimizer. These parameters usually need not to be altered. Their values are chosen in such a manner that in most cases the convergence will be sufficient. Only for very special problems, it will be necessary to change these parameters in order to improve convergence. The other dataset is the problem input file, which contains all data to describe the physical problem.

Herein first the initial laminate is given by the speci-

cation of the materials used, the layer thicknesses, the fiber orientation angles and the fiber content of volume. After the applied loads the information concerning the optimization follows. In this part, the design variables, the objective function and the design constraints are declared. In order to keep this input dataset small and clear and to avoid errors due to wrong material data all material data are taken from a special data base.

2.2 The Main Routine.

In the very short main routine only the file handling, the control of data flow and the determination of the gradients are performed. The gradients of the objective function and the constraints with respect to the design variables are evaluated by finite differences. The i -th design variable is changed very little

$$\bar{x}_i = x_i + \Delta x_i$$

and the change of the objective function and the constraint values are obtained from the formula

$$\frac{\partial W}{\partial x_i} = \frac{W(\mathbf{x} + \Delta x_i) - W(\mathbf{x})}{\Delta x_i},$$

where W means the objective function respective the constraint values, $[\mathbf{x}]$ is the set of design variables, and x_i the i -th design variable. This way of determining the gradients is a little bit costly, but as the whole theory consists only of some simple matrix operations this effort is justifiable. The advantage of this method is the simplicity and the generality in its application.

Before calling the optimizer the value of the objective function, which is delivered from the analysis module, has to be scaled. The values of the constraints are already normalized, as they are always defined by

$$g_i(\mathbf{x}) = 1 - \frac{r_{actual}(\mathbf{x})}{r_{limit}}$$

for an upper limit, respective

$$g_i(\mathbf{x}) = \frac{r_{actual}(\mathbf{x})}{r_{limit}} - 1$$

for a lower limit of the constraint g_i . r_{limit} denotes the applied limit for that constraint, r_{actual} means its actual value. These formulations imply that within the feasible domain all values of the design constraints $g(\mathbf{x})$ have to be positive:

$$g_i(\mathbf{x}) \geq 0$$

Scaling is necessary, as the optimizer sums up the values of the objective function and the constraints and as these values can be of very different magnitudes. Only with scaling, sufficient convergence can be achieved.

2.3 The Analysis Module.

In the first run of the analysis module all problem specific input and the definition of the constraints, the objective function as well as the design variables (determination of the linking matrix $[\mathbf{L}]$) are done. Beside this all problem specific calculations which do not depend on the

design variables (i.e. stiffness matrices of the unidirectional layers) are performed in order to minimize the run time. In the subsequent calls of the analysis module, this part is ignored. In the remaining code, the actual laminate analysis is performed and the values of the objective function and of the constraints are evaluated and returned to the calling main program.

Basis of this analysis module is the classical laminate theory (CLT, in detail described in many monographies, e.g. [3] and [4]), which delivers the material law of a general layered laminate in the form

$$\begin{pmatrix} n \\ m \end{pmatrix} = \begin{pmatrix} A & B \\ B & D \end{pmatrix} \begin{pmatrix} \epsilon_0 \\ \kappa_0 \end{pmatrix} - \begin{pmatrix} \alpha_f \\ 0 \end{pmatrix} \Delta T. \quad (1)$$

This material law is calculated from the data of the unidirectional layers and the information about the laminate lay-up (layer thickness and fiber orientation angle). By use of this material law the stresses in the individual unidirectional layer and the factor of safety against fiber failure and interlaminar failure can be determined. For the calculation of factors of safety the Tsai-Wu failure criterion is used.

2.4 The Optimizer.

The optimization routine PEFOP is an available routine from the Institute for Computer Applications (ICA) at the University Stuttgart (Prof. Argyris). It works with the method of the interior penalty function which is modified in such a way that the start design need not to be a feasible design. With this modification the optimizer is suited well for the application of laminate optimization.

In the method of the interior penalty function, the original optimization problem with constraints is changed into a problem without constraints by introducing a new objective function Z , which is the the original objective function Φ plus the sum of all reciprocal design constraints, weighted with a scalar factor r_k .

$$Z(\mathbf{x}) = \Phi(\mathbf{x}) + r_k \sum_{i=1}^k \frac{1}{g_i(\mathbf{x})},$$

with

$$g_i(\mathbf{x}) \geq 0.$$

Near the border of the feasible domain, the values of the active constraints are near zero and the new objective function Z will reach infinity. To find the minimum of the objective function Φ under consideration of the design constraints, it is therefore sufficient to minimize the new unconstraint objective function Z . By reducing the scalar factor r_k after every iteration, the minimum of Φ will be found. Near the optimum there may be some numerical difficulties ($Z = \Phi + 0 \cdot \infty$), but for real tasks this was never a problem.

Another optimizer was also tested in this program. It was the routine DNCONF from the IMSL library. With this optimizer, too, very good results have been achieved.

2.5 Examples for the application of OLGA.

In the following, two examples for the application of this laminate optimization code are shown. The fuselage of a new helicopter (figure 3) will be an all composite structure. Preliminary analysis delivers the loads for some typical areas of the airframe. With this data, for instance, the panel in the upper part of the helicopter sidewall can be dimensioned. This part is designed as a monolithic panel made out of carbon fiber material.

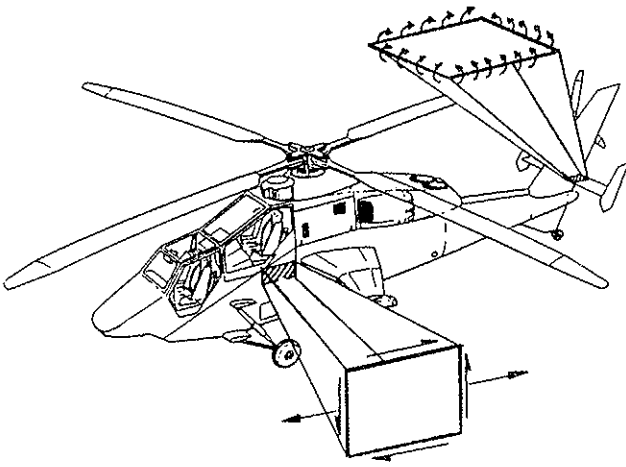


Figure 3: Helicopter fuselage

Another area of interest is the horizontal stabilizer. In the inner part of the upper sandwich panel very special loads (due to maintainance) have to be applied. With the application of OLGA the optimal sandwich configuration can be determined.

2.5.1 Tension – shear panel. The loading of the helicopter sidewall panel is shown in figure 4. For this monolithic panel, made from carbon fiber reinforced material, the following loads are given as an example:

$$\begin{aligned} n_x &= 100 \text{ [N/mm]}, \\ n_{xy} &= 100 \text{ [N/mm]}. \end{aligned}$$

The laminate shall endure these loads under consideration of fiber and matrix failure, objective function shall be the weight of the laminate. The initial laminate is a quasiisotropic lay-up with fiber orientation angles of 0° , 90° and $\pm 45^\circ$. In table 1 a summary of the optimal laminates is shown.

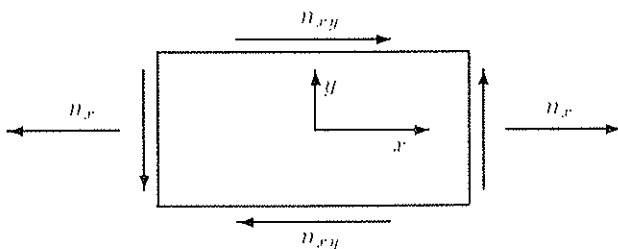


Figure 4: Panel under tension and shear

From this table it can be seen that dependent on the chosen design variables very different weights for the optimal laminates result. The quasiisotropic lay-up shall be the reference laminate.

First, the thicknesses of the three different layers (the $+45^\circ$ and the -45° layer are linked together) are design variables:

$$[\mathbf{x}] = [t_{0^\circ}, t_{90^\circ}, t_{\pm 45^\circ}]^T.$$

This results in a weight reduction of about 29% compared to the quasiisotropic lay-up. In this case, the thickness of the 90° layer reaches its lower limit (given to 0.01 mm). This shows that the 90° layer is not necessary for the load transferring. Removing this layer yields additional 3% weight saving. Allowing an anisotropic laminate (by removing the linking between the $+45^\circ$ and the -45° layer) further 15% weight can be saved. Till now, only the thicknesses of the individual layers are varied. Now, also the fiber orientation angles β shall be changed. The vector of design variables reads in this case

$$[\mathbf{x}] = [t_{0^\circ}, t_{90^\circ}, t_{\pm\beta}, \beta]^T.$$

The 5th line of table 1 shows a weight reduction of 50% for a laminate with fiber angles of $0^\circ/90^\circ/\pm 22.7^\circ$ compared to the quasiisotropic laminate. In this laminate the thickness of the 0° as well as the 90° layer have reached their lower bound (given to 0.01 mm). When these layers are removed, further 8% weight can be saved. The lightest possible laminate for the given loads is an anisotropic one with fiber orientation angles of $+32.6^\circ$ and -36.1° . This laminate has only one fourth of the mass of the quasiisotropic laminate.

From this example it can be seen that it is very useful to do such studies concerning optimal light laminates. Even if an anisotropic laminate is not desirable due to the shear – tension coupling, large weight savings can be achieved by using optimal layer thicknesses and fiber orientation angles.

2.5.2 Sandwich panel. Another example for the application of the program OLGA is the upper panel of the horizontal stabilizer of a helicopter. In the area near the fuselage the stabilizer must be walkable to enable maintainance of the tail-rotor. To fulfill this requirement the panel must withstand the following plate moments

$$m_x = m_y = 400 \left[\frac{\text{Nmm}}{\text{mm}} \right]$$

(one mechanic (80 kg) plus tools (30 kg) and an applied load factor of 1.2). The panel is designed as a sandwich with aramid fiber face sheets and a honeycomb core.

In this case the question is: what honeycomb core and what thicknesses of core and face sheets shall be chosen in order to get a panel with minimal weight. Critical failure of a sandwich, loaded in compression or bending is usually face sheet wrinkling. This failure can be taken into account as a design constraint in the laminate optimization code OLGA. To answer the above question, the

Table 1: Optimal laminates for a panel under tension and shear loads

Design Variable	Orthotropic	t_{0° [mm]	t_{90° [mm]	$+\beta$ [°]	$t_{+\beta}$ [mm]	$-\beta$ [°]	$t_{-\beta}$ [mm]	Weight [kg/m ²]	rel. Weight [%]
t	quasi	0.1449	0.1449	45.0	0.1449	45.0	0.1449	1.781	100.0
t	yes	0.0951	0.01	45.0	0.1543	45.0	0.1543	1.271	71.4
t	yes	0.0894	-	45.0	0.1541	45.0	0.1541	1.222	68.6
t	no	0.0691	-	45.0	0.1974	45.0	0.0442	0.955	53.6
t, β	yes	0.01	0.01	22.7	0.1346	22.7	0.1346	0.888	49.9
t, β	yes	-	-	35.5	0.1199	35.5	0.1199	0.737	41.4
t, β	no	-	-	32.6	0.1277	36.1	0.0279	0.478	26.8

optimal laminate (objective function is the weight, design constraints are the face sheet wrinkling and the face sheet strength) is determined for some different honeycomb cores. Preliminary studies showed that the optimal laminate of the face sheets will be a 0°/90° lay-up. Therefore the set of design variables is defined to

$$[x] = [t_{0^\circ}, t_{90^\circ}, t_{core}]^T.$$

Table 2 shows the results for a sandwich with (0°/90°) face sheets made from aramid fiber reinforced material, when fiber and matrix failure as well as face wrinkling failure are considered.

Table 2: Optimal sandwich configurations for a panel due to different honeycomb cores

ρ_{core} [kg/m ³]	E_{core} [N/mm ²]	Weight [kg/m ²]	t_{0° [mm]	t_{90° [mm]	t_{core} [mm]
24	41	1.981	0.147	0.142	19.59
32	76	1.842	0.121	0.121	17.91
48	138	2.086	0.103	0.102	21.09
64	193	2.408	0.121	0.119	17.90

It can be clearly seen that the core with a weight of 32 kg/m³ results in the lightest sandwich. Lighter cores as well as stronger cores result in heavier sandwiches. For lighter cores, face sheet wrinkling is the active constraint. But with decreasing the core stiffness, the core thickness and with it the sandwich weight has to be increased in order to reduce the force (stress) in the face sheets to achieve a sufficient factor of safety with respect to face sheet wrinkling. For stronger cores the low strength of the aramid fiber laminate in the compression direction is the active constraint. As in this case the core type has no influence on the laminate strength of the face sheets, heavier cores always result in heavier sandwiches. Figure 5 clearly shows these facts. The best compromise with respect to the weight is the sandwich with the 32 kg/m³ core.

3. Analysis of inhomogeneous bars

With the use of the fiber reinforced materials, effects become important, which often could be neglected for

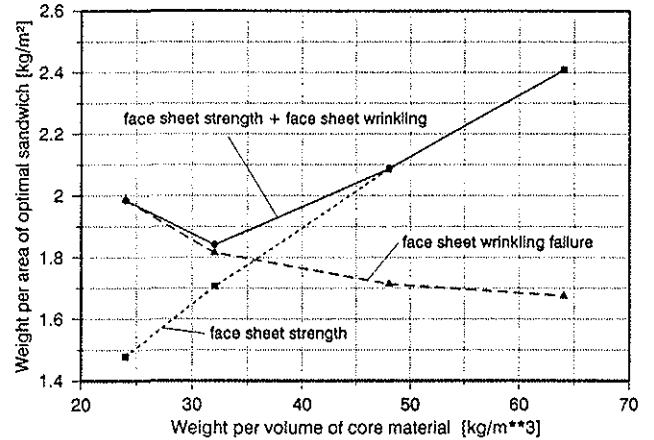


Figure 5: Weight of an optimal sandwich panel

isotropic materials. One of these effects is the influence of different Poisson's ratios in non-homogeneous barlike structures on the deformation under tension, bending and temperature loads. These barlike structures can be helicopter rotorblades, transmission shafts for the tail rotor, control links or every other bar in helicopter structures.

When loading non-homogeneous bars, the different materials want to deform independent from each other. But as they are bonded together, their deformations are restraint by the neighbouring materials (figure 6). This results in additional stresses perpendicular to the bar axis which increase the resulting bar stiffness compared to a beam where all materials have the same Poisson's ratio.

In helicopter structure analysis it is particularly important to know the exact resulting bar stiffnesses as helicopter structures are dynamically high loaded structures, whose eigenfrequencies are in tune with each other. Therefore a special theory was developed to determine the influence of restrained transverse strains on the stiffnesses. This theory allows to determine the resulting stiffnesses and coefficients of thermal expansion as well as the stresses perpendicular to the bar axis with a relatively low numerical effort. For the special geometry of a circular tube analytical solutions exist.

Mußchelischwili [5] shows a way to calculate the stiffnesses of non-homogeneous bars by using complex stress

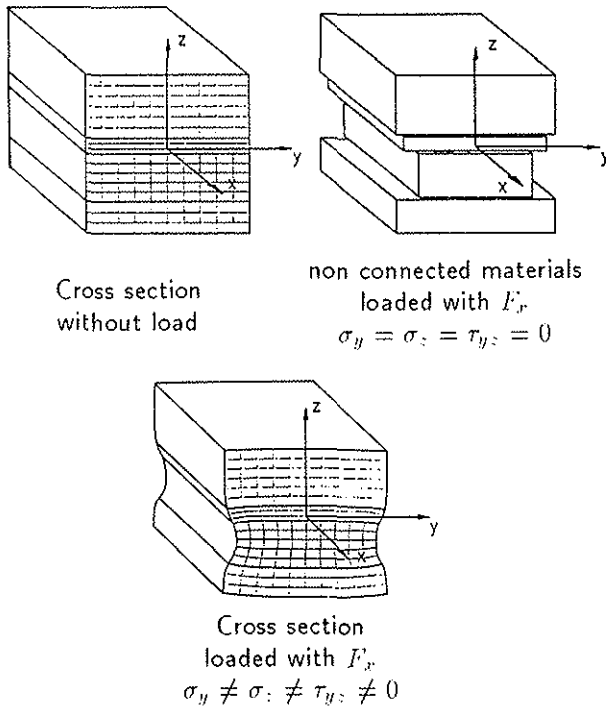


Figure 6: Non-homogeneous bar under a load in axial direction

functions. Some other authors follow his way to calculate the stresses in non-homogeneous tubes ([6], [7]). For general geometries this approach is not suited, so that in the following a theory based on the theory of finite elements is shown. The analytical solution for non-homogeneous circular tubes is described in detail in [8].

3.1 Engineering theory of bending

In the engineering theory of bending (ETB) the relation between the strain in axis direction (linear distributed over the cross section)

$$\epsilon_x = a + by + cz \quad (2)$$

and the resulting cross section loads F_x , M_y and M_z (figure 7) is given by the equation

$$\begin{pmatrix} EA & ES_x & ES_y \\ ES_x & EI & EI_y \\ ES_y & EI_y & EI_z \end{pmatrix} \begin{pmatrix} a \\ b \\ c \end{pmatrix} = \begin{pmatrix} F_x + F_{thx} \\ -M_y - M_{thy} \\ M_z + M_{thz} \end{pmatrix} \quad (3)$$

This equation is an analytical solution of the fundamental equations of the theory of elasticity (the equilibrium, the compatibility and the material law) for the one dimensional state of stress (the stress σ_x is the only non-zero stress component) and the linear strain distribution (2) over the bar cross section. The coefficients in the left matrix describe the stiffnesses of the bar:

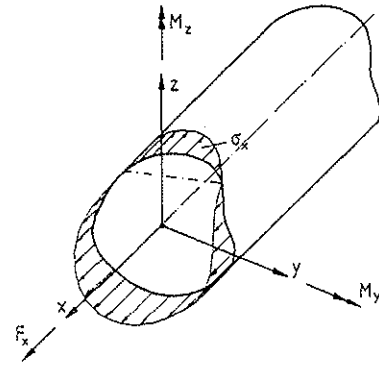


Figure 7: Definition of the resulting cross section loads

- EA : tension stiffness,
- ES_y : elastic moment about y-axis,
- ES_z : elastic moment about z-axis,
- EI_y : bending stiffness about y-axis,
- EI_z : bending stiffness about z-axis,
- EI_{yz} : bending deviation stiffness.

The thermal loads F_{thx} , M_{thy} and M_{thz} in the right vector result from a temperature difference ΔT and the coefficients of thermal expansion. With these loads the deformation of the bar under thermal loading (i.e. the strain coefficients a , b and c) can be determined.

From the stiffness coefficients and the thermal loads the position of the elastic and thermal center as well as the orientation of the principle axis can be calculated. Furthermore they allow the determination of the resulting coefficients of thermal expansion α_t and of thermal curvature κ_{ty} and κ_{tz} .

In the case of homogeneous or of non-homogeneous bars with materials, which have all the same Poisson's ratio, the stiffness coefficients and the thermal loads can be evaluated directly from the material and geometry data:

$$\begin{aligned} EA &= \int_A E dA, & EI_y &= \int_A z^2 E dA, \\ ES_y &= \int_A z E dA, & EI_z &= \int_A y^2 E dA, \\ ES_z &= \int_A y E dA, & EI_{yz} &= \int_A zy E dA. \end{aligned}$$

$$F_{thx} = \Delta T \int_A E \alpha_{tx} dA,$$

$$M_{thy} = \Delta T \int_A E \alpha_{tx} z dA,$$

$$M_{thz} = -\Delta T \int_A E \alpha_{tx} y dA.$$

Usually these stiffnesses are not only used for homogeneous bars, but also for non-homogeneous bars made from materials with different Poisson's ratios. Generally the errors are small, but if the differences in the Poisson's ratios are quite large, significant errors can occur. Therefore a more exact theory is necessary.

3.2 Three dimensional theory

From equation (3) it can be seen that it is possible to calculate the stiffness coefficients and the thermal loads from a known strain distribution (a , b and c) and the

resulting cross section loads F_x , M_y and M_z . With this the way of determining more exact stiffnesses is shown:

1. Assume a general linear strain distribution over the cross section (i.e. define the strain coefficients a , b and c from equation (2)).
2. Determine the resulting cross section loads due to this strain distribution.
3. Evaluate the stiffness and thermal coefficients by the use of equation (3).

To calculate all unknown stiffness coefficients and the thermal loads from equation (3) four independent strain distributions are necessary (e.g. tension, bending about both axis and a thermal load). The main difficulty in the application of the above way to determine the stiffnesses is item 2. For the evaluation of the resulting cross section loads conventional three dimensional calculations with the method of finite elements can be used. But this means a relatively high effort. Therefore a way is shown in the following, in which a two dimensional finite element analysis is sufficient for the determination of the special three dimensional state of stress. The resulting cross section loads then can be calculated by integrating the stress σ_x over the cross section:

$$F_x = \int_A \sigma_x dA. \quad (4)$$

$$M_y = \int_A \sigma_x z dA. \quad (5)$$

$$M_z = \int_A \sigma_x y dA. \quad (6)$$

3.3 Determination of the three dimensional state of stress.

The fundamental equation of the theory of finite elements reads ([9])

$$[\mathbf{K}][\mathbf{u}] = [\mathbf{F}] + [\mathbf{F}_{int}] \quad (7)$$

$[\mathbf{K}]$ means the stiffness matrix of the whole system. $[\mathbf{u}]$ is the vector of all gridpoint displacements. $[\mathbf{F}]$ describes the whole load vector (applied outer loads) whereas $[\mathbf{F}_{int}]$ denotes the inner loads due to a temperature difference or other inner distortions.

$[\mathbf{K}]$ is built from the element stiffness matrices $[\mathbf{k}]$. Equation (7) can be written down for only one element:

$$[\mathbf{k}][\mathbf{u}] = [\mathbf{f}] + [\mathbf{f}_{int}] \quad (8)$$

Herein the element stiffness matrix and the vector of the inner loads can be detailed:

$$\left[\int_V \mathbf{D}^T \mathbf{E} \mathbf{D} dV \right] [\mathbf{u}] = [\mathbf{f}] + \left[\int_V \mathbf{D}^T \mathbf{E} \delta dV \right]. \quad (9)$$

or, with $dV = t dA$

$$t \left[\int_A \mathbf{D}^T \mathbf{E} \mathbf{D} dA \right] [\mathbf{u}] = [\mathbf{f}] + t \left[\int_A \mathbf{D}^T \mathbf{E} \delta dA \right]. \quad (10)$$

In (10) $[\mathbf{D}]$ denotes the differential matrix from the compatibility equations,

$$[\epsilon] = [\mathbf{D}][\mathbf{u}], \quad (11)$$

$[\mathbf{E}]$ the material compliance matrix and $[\delta]$ the temperature load vector from the material law

$$[\epsilon] = [\mathbf{E}][\sigma] + [\delta]. \quad (12)$$

Equation (12) needs a further explanation: The Hooke's law for an orthotropic material is given by

$$\begin{pmatrix} \epsilon_x \\ \epsilon_y \\ \epsilon_z \\ \gamma_{xz} \\ \gamma_{zy} \\ \gamma_{xy} \end{pmatrix} = \begin{pmatrix} a_{11} & a_{12} & a_{13} & 0 & 0 & 0 \\ a_{12} & a_{22} & a_{23} & 0 & 0 & 0 \\ a_{13} & a_{23} & a_{33} & 0 & 0 & 0 \\ 0 & 0 & 0 & a_{44} & 0 & 0 \\ 0 & 0 & 0 & 0 & a_{55} & 0 \\ 0 & 0 & 0 & 0 & 0 & a_{66} \end{pmatrix} \begin{pmatrix} \sigma_x \\ \sigma_y \\ \sigma_z \\ \tau_{xz} \\ \tau_{zy} \\ \tau_{xy} \end{pmatrix} + \begin{pmatrix} \alpha_{tx} \\ \alpha_{ty} \\ \alpha_{tz} \\ 0 \\ 0 \\ 0 \end{pmatrix} \Delta T. \quad (13)$$

With a given strain distribution ϵ_x equation (13) can be reordered by introducing this strain distribution:

$$\begin{pmatrix} \epsilon_y \\ \epsilon_z \\ \gamma_{xz} \\ \gamma_{zy} \\ \gamma_{xy} \end{pmatrix} = \begin{pmatrix} b_{22} & b_{23} & 0 & 0 & 0 \\ b_{23} & b_{33} & 0 & 0 & 0 \\ 0 & 0 & a_{44} & 0 & 0 \\ 0 & 0 & 0 & a_{55} & 0 \\ 0 & 0 & 0 & 0 & a_{66} \end{pmatrix} \begin{pmatrix} \sigma_y \\ \sigma_z \\ \tau_{xz} \\ \tau_{zy} \\ \tau_{xy} \end{pmatrix} + \begin{pmatrix} \delta_{ty} \\ \delta_{tz} \\ 0 \\ 0 \\ 0 \end{pmatrix} \Delta T. \quad (14)$$

The missing stress σ_x can be calculated from the equation

$$\sigma_x = \frac{1}{a_{11}} (\epsilon_x - a_{12} \sigma_y - a_{13} \sigma_z - \alpha_{tx} \Delta T). \quad (15)$$

The stiffness coefficients b_{ij} and δ_j from (14) are defined as

$$b_{ij} = \left[a_{ij} - \frac{a_{i1} a_{j1}}{a_{11}} \right], \quad (16)$$

$$\delta_j = \left[\alpha_{tj} + \frac{a_{j1}}{a_{11}} \left(\frac{\epsilon_x}{\Delta T} - \alpha_{tx} \right) \right] \Delta T. \quad (17)$$

Equation (14) corresponds directly with equation (12), so that an applied strain distribution $\epsilon_x(y, z)$ via δ_j has some influence on the inner loads of an element. Now with the above equations it is possible to calculate the three dimensional state of stress under the assumption of non-varying stresses and strains along the beam axis by using a two dimensional finite element model. This state of strain is generally called the generalized state of plane strain.

3.4 The computer code SABINA

The above described theory is the basis of the computer code SABINA, which means Stiffness of Any Beam with

Inhomogeneous cross sections. SABINA is a finite element code, specially developed to determine bar stiffnesses and resulting coefficients of thermal expansion [10]. Moreover it can also be used to do simple two dimensional calculations, concerning the state of plane stress and the generalized state of plane strain.

As written above, the stiffness determination requires four independent strain distributions. SABINA uses the following load cases by default:

1. Only tension ($\epsilon_x = 1.0$),
2. only bending about the y-axis ($\epsilon_x = z$),
3. only bending about the z-axis ($\epsilon_x = y$),
4. only temperature load ($\Delta T = 1.0$).

Output of SABINA are the three dimensional stress distribution as well as the bar stiffnesses, the position of the elastic and the thermal center and the orientation of the principle axes. With the aid of a simple plot routine, the deformation of the cross section can be plotted for all four load cases.

All results are stored in a data base, so that it is simple to do some post processing such as a stress analysis considering all stress components or further plotting of stresses or deformations.

3.5 Examples

Two examples will show the effect of constraint transverse strain due to different Poisson's ratios. At first a special bar is considered to show the influence different Poisson's ratios can have. Second, the stiffnesses of a typical helicopter rotor blade are calculated and compared with the stiffnesses, obtained with the engineering theory of bending.

3.5.1 Special testbar. To show the influence of different Poisson's ratios, a special testbar is investigated. The bar is made out of carbon fiber reinforced material, has a quadratic cross section and a lay-up shown in figure 8.

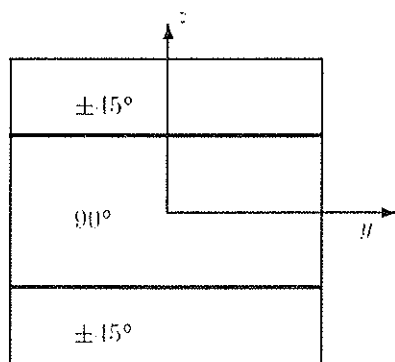


Figure 8: Cross section of the testbar

The results of this investigation are shown in the figures 9 to 11, where the stiffness respectively the coefficient of thermal expansion is plotted versus the portion of $\pm 15^\circ$ layers of the whole cross section. Additionally to

the result from the above shown theories (the engineering theory of bending and the three dimensional theory) results from the classical laminate theory are plotted. These results can be got from equation (1) by introducing $n_y = n_{xy} = m_y = m_{xy} = 0$. Then the remaining stiffness coefficients are the bar stiffnesses.

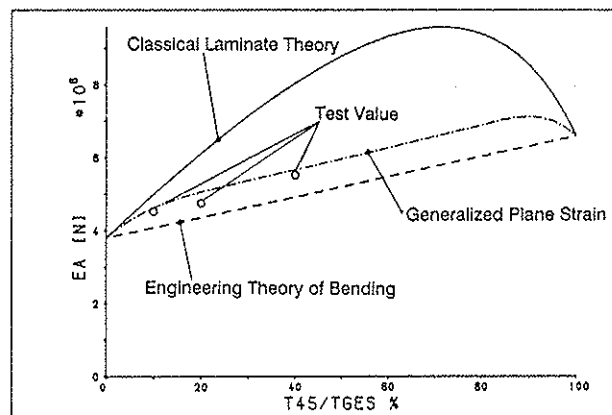


Figure 9: Tension stiffness of testbar

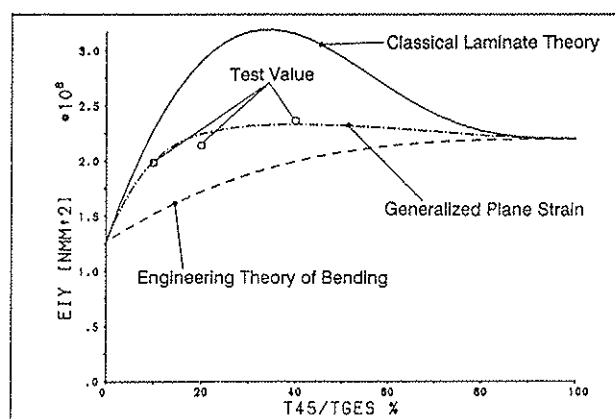


Figure 10: Bending stiffness of testbar about y-axis

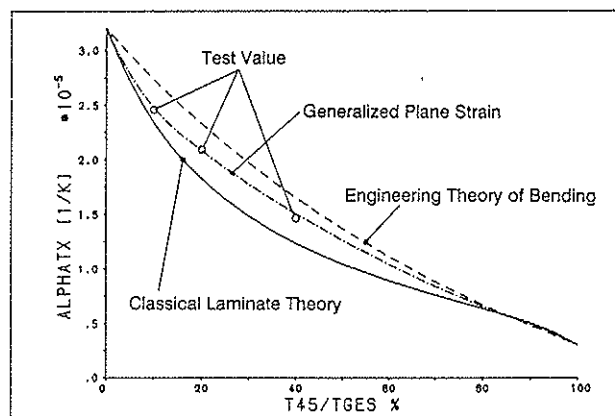


Figure 11: Coefficient of thermal expansion of the testbar

These figures show a very great influence of the constraint transverse strain due to different Poisson's ratios.

Especially the bending stiffness about the y -axis deviates very much from the real value. The reason for this is the very high stiffness of the 90° layer in the transverse direction of the bar together with the high Poisson's ratio of the $\pm 45^\circ$ layer (about 0.8). The high stiffness of the 90° layer nearly completely restrains the lateral contraction of the $\pm 45^\circ$ layer and so high additional stresses occur, which result in the stiffness increase. Test results are in good correlation with the three dimensional theory.

3.5.2 Helicopter rotor blade. In general helicopter rotor blades are very non-homogeneous barlike structures. Very different materials are used in their cross sections (figure 12) in order to meet the requirements. Metals

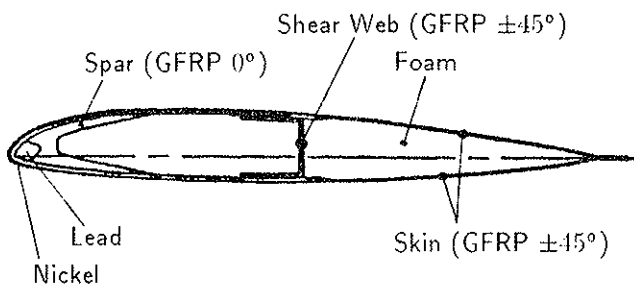


Figure 12: Cross section of a typical helicopter rotor blade

protect the blade against erosion (steel, titanium or nickel) and position the center of gravity (lead). Different fiber reinforced materials are responsible for the blade properties: $\pm 45^\circ$ laminate for high torsional stiffness and strength as well as for the shear properties; unidirectional laminates for tension and bending stiffnesses. In table 3 the material properties of different materials are given.

Table 3: Properties of materials, used in helicopter rotor blades

Material	E_1 [$\frac{N}{mm^2}$]	E_2 [$\frac{N}{mm^2}$]	G_{12} [$\frac{N}{mm^2}$]	ν_{12} [-]
Steel	210000	210000	82000	0.28
Titanium	105000	105000	39500	0.33
Nickel	197000	197000	75000	0.31
Lead	16000	16000	5600	0.44
GFRP 0°	43000	10000	7100	0.28
GFRP $\pm 45^\circ$	17000	17000	11500	0.47
GFRP $0^\circ/90^\circ$	26700	26700	5800	0.17
CFRP 0°	128000	8000	4300	0.28
CFRP $\pm 45^\circ$	12300	12300	29000	0.80
CFRP $0^\circ/90^\circ$	60000	60000	3400	0.08
Foam	100	100	36	0.40

As an example the airfoil section of a rotor blade for a helicopter of the 2 to class is investigated. In this rotor blade nickel, lead, GFRP 0° and GFRP $\pm 45^\circ$ are

the used materials. Figure 13 shows the cross section deformations due to three standard loadcases.

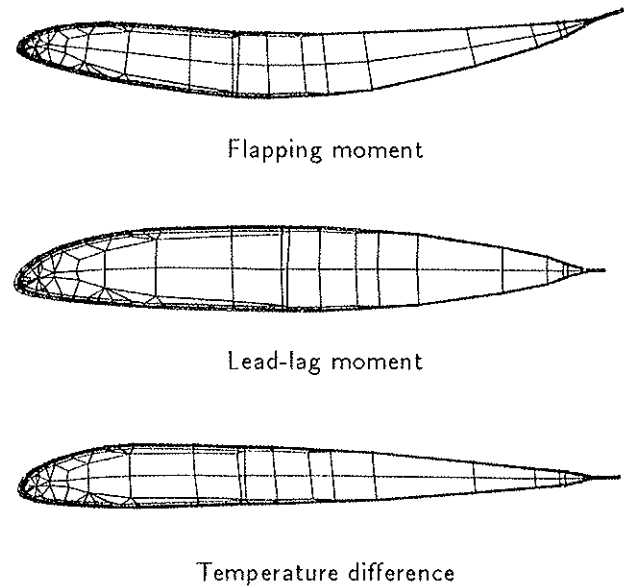


Figure 13: Deformations of a rotor blade cross section due to typical loads

In table 4 the stiffness results and the position of the elastic center are given. The differences of the stiffnesses and the coordinates of the elastic center are very small (about 2%), so that in this case the influence of different Poisson's ratios can be neglected. The reason for this is the low stiffness of the most materials (the foam and the GFRP 0°) in the transverse direction. Fortunately, this is valid for most barlike parts in helicopter structures. Nevertheless it always should be proved, whether the simpler engineering theory of bending or the more complicated theory of generalized plane strain may be applied.

Table 4: Stiffness properties of a helicopter rotor blade

Property		Engineering Theory of Bending	Generalized Plane Strain
Tension stiff.	[N]	$5.874 \cdot 10^7$	$5.194 \cdot 10^7$
Lead-lag stiff.	[Nmm^2]	$1.992 \cdot 10^{11}$	$2.011 \cdot 10^{11}$
Flapping stiff.	[Nmm^2]	$7.618 \cdot 10^9$	$7.769 \cdot 10^9$
Elast. center			
y-coord.	[mm]	60.48	60.46
z-coord.	[mm]	4.68	4.71

4. Structural analysis of thickwalled helicopter components

In modern helicopter structures more and more thick-walled structures made from fiber reinforced materials are used. Examples are for instance the plates of the rotor hub of the German-French anti-tank helicopter

PAH/HAC [1] or the load introduction areas of rotor blades. The thickness of these elements reaches up to 80 mm, the widths of single parts are in the same magnitude. Therefore these structures can no more be analysed as thinwalled plates or membranes. A real three dimensional theory must be used.

The method of finite elements is suited well for this analysis, as there exists nearly no limitation concerning the geometry. But another difficulty occurs: The material properties of general laminates are not known in three dimensions. Usually, the material properties of laminates are evaluated by using the classical laminate theory ([3], [4]), but this theory gives no information about the properties in the direction perpendicular to the laminate. To solve this difficulty, Pagano [11] made an extension of the classical laminate theory. With this extension all three dimensional properties of laminates can be calculated.

So, in finite element analysis it is no longer necessary to idealize each unidirectional layer. Several layers can be combined to one new material, for which the properties can be calculated by this theory. After analysing the structure with a finite element code, the element forces can be used to determine the three dimensional stresses in the single layers with the same theory. By applying a proper failure criterion factors of safety can be evaluated. In the future this procedure can be easily implemented in existing finite element codes as it was done with the classical laminate theory some years ago.

4.1 Extended laminate theory

In the classical laminate theory all layers are considered as connected in parallel. This means, all layers sustain the same strain (when only a tension load is applied). Due to the plane state of stress no information about the direction perpendicular to the laminate plane is necessary. In the extended theory, for this direction it is assumed that in each layer of the laminate acts the same stress. So, in thickness direction the layers are connected in series (figure 14).

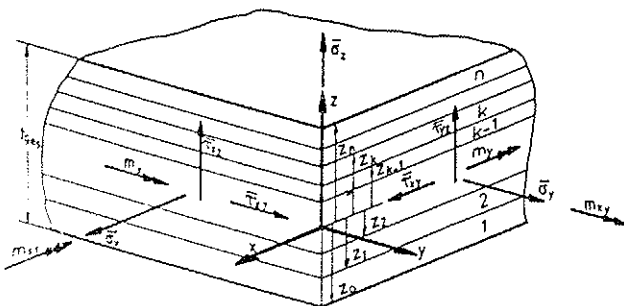


Figure 14: Definitions for a laminate

In this case it is useful not to work with forces per length, as it is usual in the classical laminate theory, but to work with the following average stresses in the x-y plane.

$$\bar{\sigma}_i = \frac{n_i}{t_{ges}}, \quad \bar{\tau}_{ij} = \frac{n_{ij}}{t_{ges}}, \quad \bar{m}_{ij} = \frac{m_{ij}}{t_{ges}}. \quad (18)$$

For the strains along the planes $x = const$ and $y = const$ the usual formulation is valid:

$$\begin{pmatrix} \epsilon_x \\ \epsilon_y \\ \gamma_{xy} \end{pmatrix} = \begin{pmatrix} \kappa_x^0 \\ \kappa_y^0 \\ \gamma_{xy}^0 \end{pmatrix} + z \begin{pmatrix} \kappa_{x,z}^0 \\ \kappa_{y,z}^0 \\ \kappa_{xy,z}^0 \end{pmatrix} \quad (19)$$

About the strains in a plane $z = const$, ϵ_z , $\gamma_{z,x}$ and $\gamma_{z,y}$ no statement is possible, but the corresponding stresses in each layer are assumed to have the same value (they are connected in series in this direction):

$$\sigma_{z,k} = \sigma_z, \quad \tau_{z,x,k} = \tau_{z,x}, \quad \tau_{z,y,k} = \tau_{z,y}. \quad (20)$$

By applying equilibrium conditions, the three dimensional material law of a laminate can be evaluated:

$$\begin{aligned} \bar{\sigma}_x &= \frac{1}{t_{ges}} \int_{z_u}^{z_o} \sigma_x dz; & \bar{m}_x &= \frac{1}{t_{ges}} \int_{z_u}^{z_o} \sigma_x z dz; \\ \bar{\sigma}_y &= \frac{1}{t_{ges}} \int_{z_u}^{z_o} \sigma_y dz; & \bar{m}_y &= \frac{1}{t_{ges}} \int_{z_u}^{z_o} \sigma_y z dz; \\ \bar{\tau}_{xy} &= \frac{1}{t_{ges}} \int_{z_u}^{z_o} \tau_{xy} dz; & \bar{m}_{xy} &= \frac{1}{t_{ges}} \int_{z_u}^{z_o} \tau_{xy} z dz. \end{aligned} \quad (21)$$

Introducing the material law of the unidirectional layers into the equations (19) and (21) and with consideration of (20) the material law of the laminate is given in the form

$$\begin{pmatrix} \bar{\sigma}_x \\ \bar{\sigma}_y \\ \sigma_z \\ \tau_{yz} \\ \tau_{zx} \\ \tau_{xy} \\ \bar{m}_x \\ \bar{m}_y \\ \bar{m}_{xy} \end{pmatrix} = \begin{pmatrix} [A] & [B] \\ [B]^T & [D] \end{pmatrix} \begin{pmatrix} \bar{\epsilon}_x \\ \bar{\epsilon}_y \\ \epsilon_z \\ \gamma_{yz} \\ \gamma_{zx} \\ \gamma_{xy} \\ \kappa_x \\ \kappa_y \\ \kappa_{xy} \end{pmatrix} - \begin{pmatrix} \bar{\sigma}_{tx} \\ \bar{\sigma}_{ty} \\ \sigma_{tz} \\ \tau_{tyz} \\ \tau_{t zx} \\ \tau_{t xy} \\ \bar{m}_{tx} \\ \bar{m}_{ty} \\ \bar{m}_{t xy} \end{pmatrix} \Delta T. \quad (22)$$

The submatrices [A], [B] and [D] have the dimensions 6 by 6, 3 by 6 and 3 by 3 respectively. The equations for evaluating the coefficients of these matrices are much more complicated than in the classical laminate theory, they are given in the appendix.

From the matrix of compliances $\begin{pmatrix} [A] & [B] \\ [B]^T & [D] \end{pmatrix}^{-1}$ the effective moduli of the laminate can be determined. These are the properties, a finite element code needs for structural analysis.

This extended theory was programmed in the computer code ETHERM3D. This code allows the determination of all three dimensional properties of laminates (i.e. Young's moduli, shear moduli, Poisson's ratios, coefficients of thermal expansion and thermal curvature). Moreover the stresses in the unidirectional layers and the corresponding factors of safety can be calculated for

given loads. So this computer code is an excellent supplement for common finite element codes.

4.2 Some three dimensional properties of laminates

In the following some unusual features of the properties in thickness direction of laminates shall be shown. In the figures 15 and 16 the moduli of elasticity and the coefficient of thermal expansion of a $\pm\beta$ laminate (CFRP, fiber T300, fiber volume content 60%) in the direction perpendicular to the laminate plane is plotted versus the angle β .

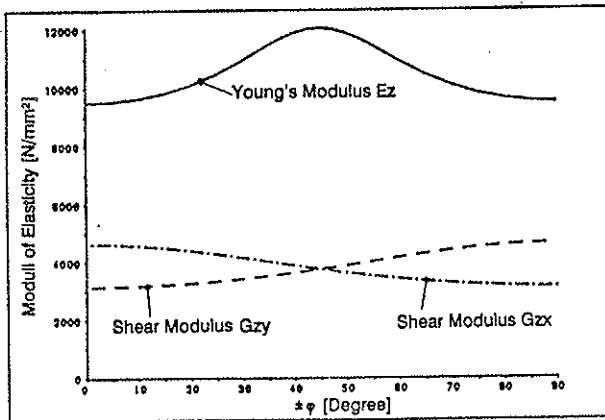


Figure 15: Moduli of elasticity in thickness direction of a $\pm\beta$ CFRP laminate

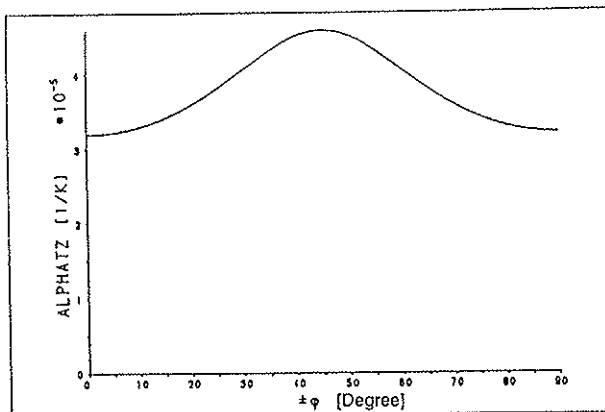


Figure 16: Coefficient of thermal expansion in thickness direction of a $\pm\beta$ CFRP laminate

Both figures show a maximum at angles β of 15° . This results from the very different stiffnesses and Poisson's ratios of the unidirectional layers in the longitudinal and in the transverse direction. The strains of the individual layer in the transverse direction is most restraint when the angle between the fibers of neighbouring layers is 90° (which means the angle β is 15°).

Figure 17 shows the Poisson's ratio in thickness direction of a $\pm\beta$ laminate, when it is loaded in the inplane direction. For relative small angles β , the Poisson's ratio reaches negative values, which is very unusual for a common material.

The above shown laminate properties in the thickness

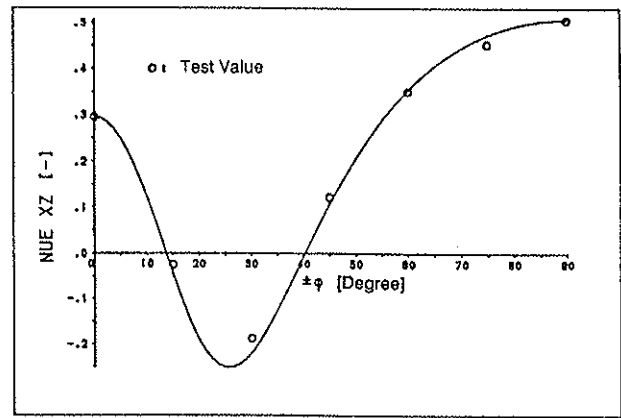


Figure 17: Poisson's ratio in thickness direction of a $\pm\beta$ CFRP laminate

direction emphasize that it is important to use the real three dimensional properties in a finite element analysis to get the correct results.

4.3 Application of ETHERM3D

Thickwalled fiber reinforced structures are used at helicopters mainly for dynamically highly loaded rotor components. So, the rotor blades themselves and especially their load introduction elements are made of these materials. Flexbeams are only possible through the extensive use of fiber reinforced materials. Figures 18 and 19 show the flexbeam and the three dimensional finite element model of the rotor blade of the BO 108 [2].

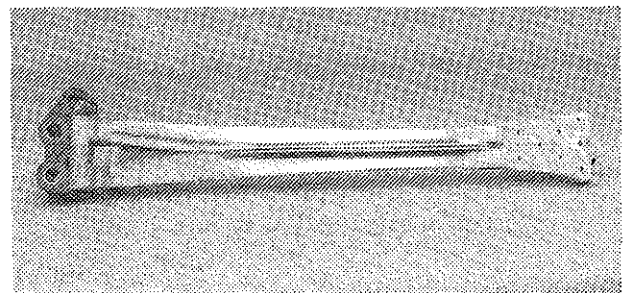


Figure 18: Flexbeam of a modern helicopter

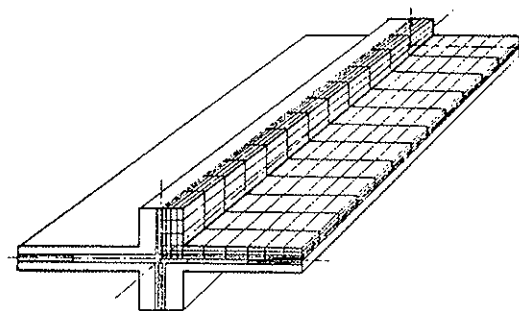


Figure 19: 3D-idealization of the flexbeam

At the German-French PAH/HAC helicopter [1], the essential components of the rotor hub are made out of fiber reinforced material. Figure 20 shows this rotor hub with the two thick CFRP plates. These plates are really three dimensional structures. Load introduction and the

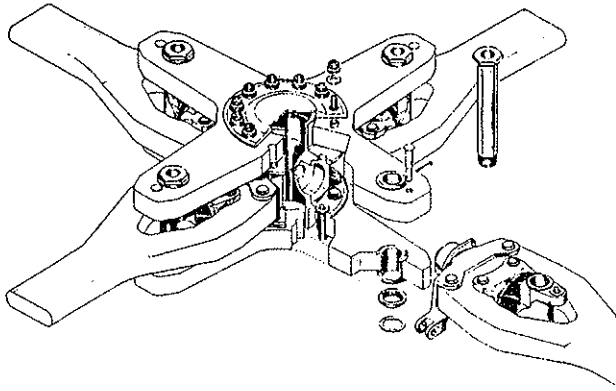


Figure 20: Rotor hub with elastomeric bearings

load paths are so complicated that with simpler models the results are unsatisfactory. In figure 21 the finite element idealization of this hub is shown. The results of this analysis are in good correlation with test results.

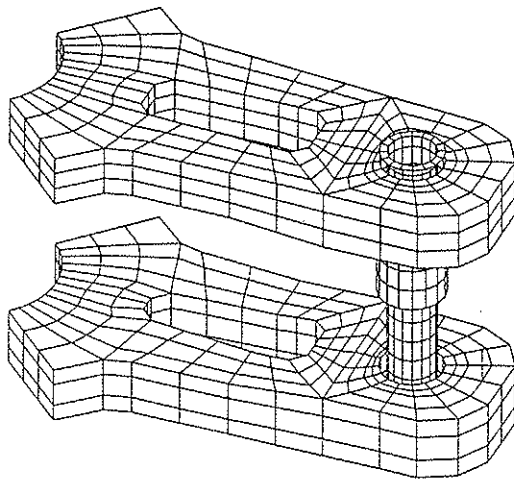


Figure 21: 3D-idealization of the rotor hub

5. Summary

The basing theory and the application of three new developed computer codes are shown. These computer codes have been created to support the process of designing helicopter structures in a very efficient way.

The computer code OLGA, based on the classical laminate theory and on procedures of the numerical optimization, allows to design optimal laminates in a very general sense. As objective functions and design constraints any result or any combination of results of the classical laminate theory can be chosen. Design variables may be the thickness and the fiber orientation angles of the unidirectional layers. Some examples show the usefulness of this program, especially in early design phases.

In the analysis of non-homogeneous bars there are some difficulties, if the materials have different Poisson's ratios. Though their influence is usually very small, in some cases they may have a noticeable influence on the bar stiffnesses and the coefficient of thermal expansion.

The computer code SABINA enables the engineer to consider this influence and to determine the real stiffnesses.

Analysis of thickwalled composite structures requires a three dimensional finite element analysis. As input data, all three dimensional properties of the used laminates are necessary. The usual classical laminate theory delivers the inplane properties only, the out-of-plane properties are unknown. The computer code ETHERM3D allows to determine all three dimensional properties as well as the stresses in single unidirectional layers due to applied outer loads (forces, moments or temperature). So, it is a very useful complement to common finite element codes, which have no such extension at this time.

References

- [1] J.C. Arribat and K. Schymanietz. HAP - PAH/HAC program. *Vertiflite*, 34(6):56, Nov. 1988.
- [2] H.B. Huber and C. Schick. MBB's BO108 design and development. 46th Annual Forum & Technology Display of the American Helicopter Society, Washington D.C., May 21 - 23 1990.
- [3] S.W. Tsai and H.T. Hahn. *Introduction to Composite Materials*. Technomic Publishing Co., Westport Conn., 1980.
- [4] B.D. Argarwal and L.J. Broutman. *Analysis and Performance of Fibre Composites*. Wiley Interscience, New York, 1980.
- [5] N.I. Mußchelischwili. *Einige Grundaufgaben zur mathematischen Elastizitätstheorie*. Carl Hanser Verlag, München, 1971.
- [6] K.H. Lo. *Bending of Laminated Beams*. PhD thesis, New York, 1973.
- [7] R.D. Shile. A non-homogeneous beam in plane stress. *Journal of Applied Mechanics*, page 582. Sept. 1960.
- [8] H. Rapp. Inhomogene Kreisrohre unter Zug-, Temperatur- und reiner Biegebeanspruchung. *Ingenieur Archiv*, 60:225, 1990.
- [9] O.C. Zienkiewicz. *Methode der finiten Elemente*. VEB Fachbuchverlag, Leipzig, 1975.
- [10] H. Rapp. *Inhomogene Balken unter Temperatur-, Zug- und reiner Biegebeanspruchung*. PhD thesis, Technische Universität München, 1988.
- [11] N.J. Pagano. Effective moduli of composite laminates. In L.J. Broutman and R.H. Krock, editors. *Composites Materials, Volume 2*, page 25. Academic Press, New York, 1974.

APPENDIX

Equations for the determination of the stiffness coefficients for the extended laminate theory:

With the following arrangement for the indices

$$\begin{aligned} l, m &= 1, 2, 3, \\ i, j &= 1, 2, 3, 4, 5, 6, \\ K, L &= 3, 4, 5, \\ r, s &= 1, 2, 6, \end{aligned} \quad (23)$$

and the abbreviations

$$\begin{aligned} [C_{K,L}] &= \left[\sum_{k=1}^n [a_{K,L}]_k (z_k - z_{k-1}) \right]^{-1}, \\ [E_{i,L}] &= \sum_{k=1}^n [a_{i,L}]_k^{-1} [a_{K,L}]_k (z_k - z_{k-1}), \\ [F_{K,j}] &= \sum_{k=1}^n [a_{K,L}]_k [a_{K,j}]_k^{-1} (z_k - z_{k-1}), \\ [G_{r,L}] &= \frac{1}{2} \sum_{k=1}^n [a_{r,L}]_k^{-1} [a_{K,L}]_k (z_k^2 - z_{k-1}^2), \\ [H_{K,s}] &= \frac{1}{2} \sum_{k=1}^n [a_{K,L}]_k [a_{K,s}]_k^{-1} (z_k^2 - z_{k-1}^2), \\ [S_i]_k &= [a_{i,j}]_k^{-1} [\alpha_{ti}]_k, \end{aligned} \quad (24)$$

the equations for the coefficients of the submatrices of equation (22) are given by:

$$\begin{aligned} [A_{i,s}] &= \frac{1}{t_{ges}} \left[\sum_{k=1}^n [a_{i,L}]_k^{-1} (z_k - z_{k-1}) + [E_{i,L}] [C_{K,L}] [F_{K,j}] - \right. \\ &\quad \left. - \sum_{k=1}^n [a_{i,L}]_k^{-1} [a_{K,L}]_k [a_{K,j}]_k^{-1} (z_k - z_{k-1}) \right], \\ [A_{i,L}] &= [E_{i,L}] [C_{K,L}], \\ [B_{i,m}] &= \frac{1}{2t_{ges}} \left[\sum_{k=1}^n [a_{i,s}]_k^{-1} (z_k^2 - z_{k-1}^2) + [E_{i,L}] [C_{K,L}] \sum_{k=1}^n [a_{K,L}]_k [a_{K,s}]_k^{-1} (z_k^2 - z_{k-1}^2) - \right. \\ &\quad \left. - \sum_{k=1}^n [a_{i,L}]_k^{-1} [a_{K,L}]_k [a_{K,s}]_k^{-1} (z_k^2 - z_{k-1}^2) \right], \\ [D_{l,m}] &= \frac{1}{t_{ges}} \left[\frac{1}{3} \sum_{k=1}^n [a_{r,s}]_k^{-1} (z_k^3 - z_{k-1}^3) + [G_{r,L}] [C_{K,L}] [H_{K,s}] - \right. \\ &\quad \left. - \frac{1}{3} \sum_{k=1}^n [a_{r,L}]_k^{-1} [a_{K,L}]_k [a_{K,s}]_k^{-1} (z_k^3 - z_{k-1}^3) \right], \end{aligned} \quad (25)$$

$$\begin{aligned} [\sigma_{ti}] &= \frac{1}{t_{ges}} \left[\sum_{k=1}^n [S_{ti}]_k (z_k - z_{k-1}) + [D_{i,L}] [C_{K,L}] \sum_{k=1}^n [a_{K,L}]_k [S_K]_k (z_k - z_{k-1}) - \right. \\ &\quad \left. - \sum_{k=1}^n [a_{i,L}]_k^{-1} [a_{K,L}]_k [S_K]_k (z_k - z_{k-1}) \right], \\ [\overline{m}_{ti}] &= \frac{1}{t_{ges}} \left[\frac{1}{2} \sum_{k=1}^n [S_{tr}]_k (z_k^2 - z_{k-1}^2) + [G_{i,L}] [C_{K,L}] \sum_{k=1}^n [a_{K,L}]_k [S_K]_k (z_k - z_{k-1}) - \right. \\ &\quad \left. - \frac{1}{2} \sum_{k=1}^n [a_{r,L}]_k^{-1} [a_{K,L}]_k [S_K]_k (z_k^2 - z_{k-1}^2) \right]. \end{aligned} \quad (26)$$